Effect of temperature on the vibrational density of states in vitreous SiO_2: A Raman study

S. Caponi,[1,2] A. Fontana,[1,2] F. Rossi,[1,2] G. Baldi,[3] and E. Fabiani[4]
[1]*Dipartimento di Fisica, Università di Trento, via Sommarie 14, 38050 Povo, Trento, Italy*
[2]*CRS SOFT-INFM-CNR, Università di Roma La Sapienza, I-00185, Roma, Italy*
[3]*CRS SOFT-INFM-CNR, OGG, ESRF, Beamline ID16, BP220, F-38043 Grenoble Cedex 9, France*
[4]*CEA LETI Minatec, Département des Technologies pour la Biologie et la Santé, Grenoble Cedex 9, France*
(Received 2 February 2007; published 12 September 2007)

Raman scattering measurements of vitreous SiO_2 were performed over a wide range of temperatures in order to study the behavior of the boson peak and the quasielastic scattering. The analysis of quasielastic contribution in the framework of the Jäckle model demonstrates that the quasielastic excess and the acoustic attenuation have the same physical origin. Moreover and even more importantly we found that the boson peak decrease, which is observed at increasing temperature, is fully explained by the modification of the elastic constants.

DOI: 10.1103/PhysRevB.76.092201 PACS number(s): 63.50.+x, 67.40.Fd, 61.43.Fs

The vibrational dynamics of amorphous solids and glasses have been extensively studied in the last three decades.[1] Inelastic light and neutron scattering represent the principal techniques used to probe the vibrational properties in these systems. Although the main features of the spectra are now understood, some aspects are not fully explained, and these include the quasielastic scattering (QES), present in the Raman and neutron experiments of glasses,[2–9] and the temperature behavior of the boson peak (BP) intensity below the glass transition temperature.[10–13] We have focused our study on these features performing Raman scattering measurements on vitreous silica (v-SiO_2, T_g=1500 K) in a wide range of temperatures (10–1200 K) extending the temperature range hereafter reported in the literature. The low-frequency Raman scattering ($\omega < 100$ cm^{-1}) presents two main features: the BP and a broad quasielastic line, which extends beyond the Brillouin lines.[4,7] The term QES is normally associated with a broadening of the elastic line (Rayleigh wing) rather than to discrete inelastic events. It dominates the spectra of glasses at frequencies below 20 cm^{-1} and exhibits a characteristic temperature dependence. In fact the intensity of QES from 5 K up to room temperature increases more rapidly than the BP, which follows the Bose-Einstein statistics. The different temperature dependence can be used to separate the QES from the low-frequency tail of the BP. This approach has the obvious advantage to be independent, for instance, from the extrapolation of the BP to low frequency. This extrapolation, based on the ω^2 dependence of the Debye density of states, is affected by an arbitrary proportionality constant in the Raman spectrum. On the contrary the depolarization ratio $\rho(\omega)$, i.e., the ratio of depolarized (I_{HV}) to polarized (I_{VV}) Raman spectra, changes little from QES and BP and it cannot be used to separate the two contributions.

As suggested in the literature[7,14] the QES could be the result of incoherent scattering by defects that relax via thermal activation. These defects should be the same invoked to explain the ultrasonic attenuation at $T > 30$ K. The two level states can couple to light by a direct or indirect coupling mechanism.[5,7,14,15] Jäckle[15] demonstrated explicitly the relationship between the QES intensity and the sound attenuation discussing the effects of the two different coupling mechanisms. The model predicts the QES intensity vs temperature to have the same shape of the acoustic attenuation, i.e., the shape of the β relaxation: a rapid increase of the intensity up to some temperature T_0 and a decrease for higher temperatures.

Even the BP, above 300 K, has a peculiar temperature dependence. Its maximum shifts to higher frequencies and its intensity decreases with increasing temperature.[10] This behavior is observed in both Raman and neutron scattering experiments.[10] While the BP shift has been tentatively ascribed to the presence of fourth-order anharmonicity in the next-nearest-neighbor interaction potential,[10,11] there is no quantitative explanation of the decreasing of the BP intensity, especially above 500 K.

In this work we test the prediction of the model of QES intensity and we assess the origin of the BP intensity decrease, reporting detailed Raman scattering measurements, new and reanalyzed old ones. We find that the QES arises from the same mechanisms that cause the acoustic attenuation, in good agreement with the predictions of the models, and that the BP decrease is only apparent and due to the changes of the elastic constants. Raman scattering experiments were done using a standard experimental setup Jobin Yvon U1000 in a wide frequency range (from 3 to 3000 cm^{-1}), in order to correctly subtract the underlying weak background of luminescence.[16] The light polarizations were perpendicular (VV) and orthogonal (HV) to the scattering plane. The v-SiO_2 sample was a commercial spectrosil, purchased from SILO (Florence, Italy).

Figure 1 shows the depolarized reduced intensity

$$I^{\mathrm{red}}(\omega,T) = \frac{I^{HV}}{\omega[n(\omega,T)+1]} \tag{1}$$

measured on v-SiO_2, where $n(\omega,T)+1$ is the Bose-Einstein population factor. The spectra are normalized at the high-frequency peaks, as shown in the inset of the upper panel of Fig. 1. The spectra show the BP, peaked at ~50 cm^{-1}, and the QES. The lower panel shows that, increasing temperature up to room temperature, there is no intensity variation in the BP frequency range. On the contrary, a strong increase of the scattering is observed at the lower frequency. Above room

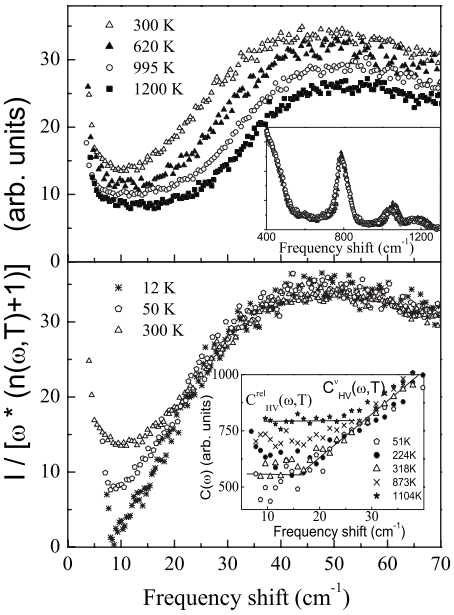

FIG. 1. Reduced Raman spectra at different temperatures: lower panel up to 300 K, upper panel up to 1200 K as shown in the figure legends. Some spectra were previously presented in Ref. 6. In the inset of the upper panel, as normalization example, we report the spectra at $T=300$, 600, 995 K. In the inset of the lower panel the low-frequency part of $C(\omega,T)_{HV}$ (Ref. 10) at some temperatures is shown. The lines are guides for the eyes, that show the temperature and frequency behavior of C_{HV}^{ν} and C_{HV}^{rel} introduced in Eq. (4).

temperature (upper panel) the scenario is completely different. Here, increasing temperature, the QES decreases and the BP shows both a shift to higher frequency and an intensity decrease.

First, we would like to discuss the results related to the BP. As reported in the literature the shift can be tentatively ascribed to a next-nearest-neighbor fourth-order anharmonicity.[10] These anharmonic effects produce a deformation of the acoustic branches and hence a shift of the BP at higher frequency. The reduced intensity is given by[10]

$$I^{\mathrm{red}}(\omega,T)=\frac{C(\omega,T)g(\omega)}{\omega^2}, \tag{2}$$

where $C(\omega,T)$ is the light vibration coupling function; when the plateau in the density of states, $g(\omega)$ (corresponding to the BP in the spectra), shifts to higher frequency, the division by ω^2 in Eq. (2) causes an artificial decrease of the peak intensity. As a numerical example, at 300 K the intensity of the maximum is divided by $(40\ \mathrm{cm}^{-1})^2$ while at 1200 K the intensity is divided by $(50\ \mathrm{cm}^{-1})^2$. To take into account this effect we have rescaled the frequency of the spectra (squeezing frequency) taken at different temperatures as $\nu=\omega/\omega_{\mathrm{BP}}(T)$.

From Eq. (2), $g(\omega)=I^{\mathrm{red}}(\omega,T)\omega^2/C(\omega)$ where $C(\omega)$ in the BP region is temperature independent and proportional to ω, $C(\omega)\sim\omega$.[10] Imposing the conservation of the total number of vibrational states, $g(\nu)d\nu=g(\omega)d\omega$, the intensity is then rescaled as

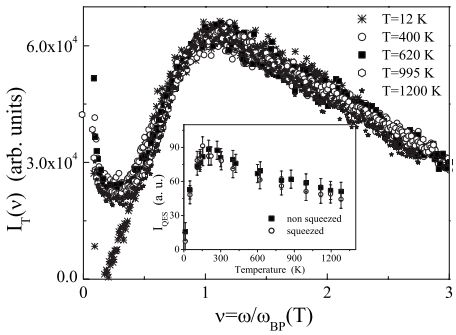

FIG. 2. Squeezed intensity obtained as described in the text as a function of the rescaled frequency $\nu=\omega/\omega_{\mathrm{BP}}(T)$. In the inset the QES intensity at 9.5 cm^{-1}, obtained both on the squeezed and non-squeezed spectra, is shown. Note that the small differences are within experimental errors.

$$I_T(\nu)=I^{\mathrm{red}}(\omega,T)\frac{\omega^2}{\nu^2}=I^{\mathrm{red}}(\omega,T)\omega_{\mathrm{BP}}^2(T). \tag{3}$$

The obtained data are reported in Fig. 2. Scaling the abscissae, the spectra rescale one on the other *without any adjusting parameter*. A master curve, whose existence is also expected by theoretical predictions,[18] is obtained.

These findings demonstrate that the decreasing of the intensity is only due to the changes in the elastic constants, which generate a BP shift. Our results are also consistent with the ideas suggested by nuclear inelastic scattering data on densified glasses[19] where the decreasing of the BP intensity was fully described by the pressure dependence of the elastic constants.

In our case, one could compare the BP shift with the sound velocity $v(T)$, but it is well known (see Ref. 11) that it exists in v-SiO_2, a different temperature dependence between the frequency position of the low q (Debye) and high q excitations.[20–22] This indicates that the temperature dependence of the acoustic modes dispersion relation is deformed, in a wide q range, from a simple linear law.

In the following, we describe the QES by the coupling of light to structural defects characterized by two configurational states. This coupling can be direct or indirect;[5,15] recently Sokolov *et al.*[5] have reported convincing results on v-SiO_2 and polystyrene in favor of the indirect mechanism. Substantially, according to this hypothesis, the contribution to the light scattering comes from the mechanical coupling of defects to the sound waves.

The ultrasonic data, in particular the bump occurring between 30 and 300 K, have been successfully interpreted in terms of relaxations of such defects. So it becomes natural to connect QES and acoustic attenuation measurements as already reported in the literature.[7,14,15] The reduced intensity described by Eq. (2) takes into account only the vibrational density of states. To describe the full spectrum, Eq. (2) must to be modified as superposition of two contributions,

$$I^{\mathrm{red}}(\omega,T)\propto C_{HV}^{\nu}(\omega,T)\frac{g(\omega)}{\omega^2}+C_{HV}^{\mathrm{rel}}(\omega,T)L(\omega,T). \tag{4}$$

Here ν indicates the vibrational part, and rel the relaxation part. In Eq. (4), the QES contribution is described by the function $L(\omega,T)$, which is given by[15]

$$L(\omega,T) \propto \int dVP(V)\frac{\tau(V)}{1+\omega^2\tau(V)^2}, \tag{5}$$

where τ is the relaxation time for potential barriers of height V, and $P(V)$ is the distribution of barrier heights. The second part of Eq. (4) shows the relationship between the QES intensity and the sound attenuation. $L(\omega)$ is proportional to $l_{rel}^{-1}(\omega)/\omega^2$ where $l_{rel}^{-1}(\omega)$ is the inverse mean free path. Hence the temperature dependence of the QES has the form of the ultrasonic attenuation. The spectral shape and the temperature variation of the coupling function is required in order to test the model predictions [see Eq. (4)]. Depending on the used model, it has been assumed $C(\omega,T)_{HV} \propto \omega^2$ (Ref. 23) or $C(\omega,T)_{HV} \sim$ constant.[24] In this work, we do not assume any temperature or frequency dependence, but we use $C(\omega,T)_{HV}$ experimentally determined. On the experimental side one can extract the coupling function by measurements of specific heat[25] or by the comparison between Raman and neutron scattering measurements.[10] Using this last procedure we have $I_R^{HV}/I_N = C_{HV}(\omega,T)$ (Refs. 10 and 26) where the indexes N and R stand for neutron and Raman, respectively. This ratio is shown in the inset of Fig. 1 at some significant temperatures. The coupling functions $C_{HV}^{\nu}(\omega,T)$ and $C_{HV}^{\mathrm{rel}}(\omega,T)$, introduced in Eq. (4), are generally unknown; however at high temperature and low frequency, where the QES dominates, $C_{HV}^{\mathrm{rel}}(\omega,T)$ is the dominant contribution of $C(\omega,T)_{HV}$: it is almost constant in frequency and its amplitude is temperature dependent. On the contrary, $C(\omega,T)_{HV}$, at higher frequencies (grater than 20 cm^{-1}), is dominated by $C_{HV}^{\nu}(\omega,T)$ that is temperature independent. Similar results were also found in other glassy systems as reported in Ref. 17.

From the Raman spectra we have obtained the scattered intensity as a function of temperature at 9.5 cm^{-1} and 13 cm^{-1} integrating the signal in a frequency window of 1 cm^{-1}. The temperature dependence is shown in the inset of Fig. 2 (full squares): we note a rapid increase up to $T \sim 170$ K, then a slow decrease at higher temperatures. The data have the form of the ultrasonic attenuation curves as predicted in Refs. 14 and 15. One could expect that the BP temperature behavior (shifting and intensity decreasing) influences the intensity at 9.5 cm^{-1} and 13 cm^{-1}, but its contribution is weak as shown in the inset of Fig. 2. Here the comparison between the QES intensity obtained, in the same spectral window, by nonsqueezed and squeezed spectra is reported. The differences are within the experimental error and in the following we report the nonsqueezed data. We conclude that the differences in the inelastic signal are essentially due to changes in the QES. Once one has recognized this effect, it is even more striking to take into account the modification induced by the temperature behavior of the coupling function. So the reduced intensity has been divided by $C(\omega,T)_{HV}$. According to Eq. (4) this quantity corresponds directly to $L(\omega)$. In order to compare our data with those obtained by the acoustic attenuation, we consider the internal friction, Q^{-1}. It is related to the inverse mean free path by $Q^{-1} \propto l^{-1}(\omega)/\omega$, so that $Q^{-1} \propto L(\omega)\omega$. Figure 3 thus presents the quasielatic intensity as the quantity $I_{\mathrm{QES}}^{*} = \omega L(\omega) = I/[n(\omega)+1]$, usually known as the imaginary part of the susceptibility function $\chi''(\omega)$, together with the acoustic attenuation data. The continuous lines are computed using a distribution of barrier heights in the thermally activated relaxation process (TARP) of Eq. (5):

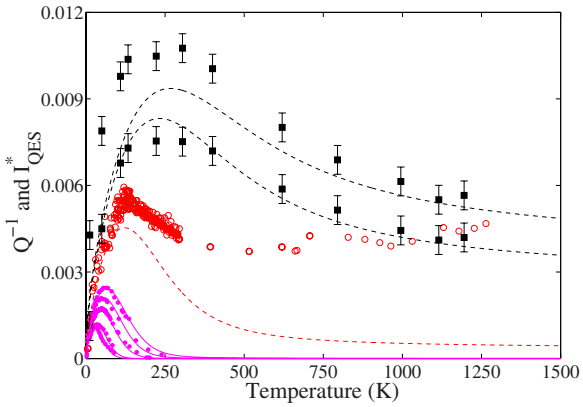

FIG. 3. (Color online) Temperature dependence of the acoustic attenuation data from ultrasonic and Brillouin measurements (full and open circles respectively). Ultrasonic measurements are acquired at 11.4 KHz (Ref. 27), 180 KHz (Ref. 28), 21 MHz (Ref. 29), 207 MHz (Ref. 30), 748 MHz (Ref. 31) (from bottom to top); the open symbols are obtained by Brillouin measurements at 33 GHz (Ref. 32). The full squares show the I_{QES}^{*} at $\omega^{*}=9.5$ cm^{-1} (285 GHz) and $\omega^{*}=13$ cm^{-1} (390 GHz) from bottom to top, respectively. The I_{QES}^{*} data are obtained as $I_{\mathrm{QES}}^{*}(T)=aI_{\mathrm{QES}}(T)\omega^{*}$ where a is the unique constant used to rescale the QES data. The continuous lines are the best-fitting functions to ultrasonic data sets with the TARP model. The dashed lines are the extrapolation to the frequencies of the I_{QES}^{*} points.

$$P(V) = \left(\frac{V}{\sigma_V}\right)^{(-\chi)} e^{-V^2/2\sigma_V^2}. \tag{6}$$

This distribution, first introduced by Keil *et al.*,[28] allows a better fit of the ultrasonic internal friction at high temperatures compared to a simple Gaussian distribution.[28] The lines in Fig. 3 are obtained with the following parameters of the model: $\tau_0 = 1.3 \times 10^{-14}$ s, $\sigma_V = 770$ K, $\chi = 0.39$. These parameters have been obtained from a multiple fit of the ultrasonic attenuation data at five different frequencies.[33] For comparison, in Fig. 3, the temperature dependence of Q^{-1} measured by Brillouin light spectroscopy[30,32] together with the extrapolation of the TARP at that frequency are reported. Although the general dependence of the Brillouin and the ultrasonic attenuation are similar, there exists disagreement with respect to the position and the amplitude of the maximum. The reason for this discrepancy is debated,[33,34] but is outside the scopes of the present work.

The QES intensity at 9.5 and 13 cm^{-1} are normalized, by the same scaling factor, on the calculated Q^{-1}. As evident from the data, there is a good *qualitative* agreement between the temperature behavior of I_{QES}^{*} and extrapolation of the TARP from ultrasonic data to hundreds of GHz. Moreover the I_{QES}^{*} at high temperature decreases while from the data at 33 GHz, one could expect a slight increase: this seems to indicate that QES is not sensible to such anharmonic effects.

It is worth to notice that, outside the experimental errors, the resulting extrapolation to 390 GHz remains constantly below the QES intensity. It could be thought that it is due to the complicated procedure in obtaining I^{*}_{QES}. A better explanation is that the difference could be associated to a static contribution to the acoustic attenuation. There are recent experimental results on v-SiO_2 (Refs. 33, 35, and 36) and v-GeO_2,[37], and theoretical ones[38] demonstrating the onset of a significant static contribution to the sound attenuation at frequency of 100–200 GHz. In this scenario the observed behavior of the QES is produced by damping due both to relaxations (temperature dependent) and static processes. The Schirmacher and co-workers theory[38] predicts a relation between the BP excess and the sound attenuation: here, we find that also the QES is strictly connected to the sound attenuation.

The main conclusions of the presented results are (i) the intensity decrease of the BP at increasing temperature is fully explained by the elastic constants modifications; (ii) a good agreement between acoustic attenuation data due to relaxations and the QES intensity is found demonstrating the same physical origin of these features.

This work was partially supported by PRIN Contract No. 2005023051 funded by MIUR.

[1] *10th International Workshop on Disordered Systems*, edited by A. Fontana, P. Verrocchio and G. Viliani [Philos. Mag. **87** (2007)].
[2] U. Buchenau, H. M. Zhou, N. Nucker, K. S. Gilroy, and W. A. Phillips, Phys. Rev. Lett. **60**, 1318 (1988).
[3] A. Fontana, F. Rocca, and M. P. Fontana, Phys. Rev. Lett. **58**, 503 (1987); A. Fontana, F. Rocca, M. P. Fontana, B. Rosi, and A. J. Dianoux, Phys. Rev. B **41**, 3778 (1990).
[4] G. Carini, G. DAngelo, G. Tripodo, A. Fontana, A. Leonardi, G. A. Saunders, and A. Brodin, Phys. Rev. B **52**, 9342 (1995).
[5] A. P. Sokolov *et al.*, Europhys. Lett. **38**, 49 (1997); J. Wiedersich, N. V. Surovtsev, V. N. Novikov, E. Rossler, and A. P. Sokolov, Phys. Rev. B **64**, 064207 (2001).
[6] A. Fontana *et al.*, J. Non-Cryst. Solids **351**, 1928 (2005).
[7] G. Winterling, Phys. Rev. B **12**, 2432 (1975).
[8] V. N. Novikov *et al.*, Europhys. Lett. **57**, 838 (2002).
[9] J. Wiedersich, S. V. Adichtcher, and E. Rossler, Phys. Rev. Lett. **84**, 2718 (2000).
[10] A. Fontana *et al.*, Europhys. Lett. **47**, 56 (1999).
[11] C. Masciovecchio *et al.*, Philos. Mag. A **79**, 2013 (1999).
[12] U. Buchenau, M. Prager, N. Nucker, A. J. Dianoux, N. Ahmad, and W. A. Phillips, Phys. Rev. B **34**, 5665 (1986).
[13] V. L. Gurevich, D. A. Prashin, and H. R. Schober, Phys. Rev. B **67**, 094203 (2003).
[14] K. S. Gilroy and W. A. Phillips, Philos. Mag. B **43**, 735 (1981); W. A. Phillips, Rep. Prog. Phys. **50**, 1657 (1987).
[15] N. Theodorakopoulos and J. Jäckle, Phys. Rev. B, **14**, 2637 (1976); J. Jäckle, in *Amorphous Solids-Low Temperature Properties*, edited by W. A. Phillips, Topics in Current Physics Vol. 24 (Springer-Verlag, Berlin, 1981), p. 135.
[16] A. Fontana *et al.*, J. Non-Cryst. Solids **352**, 4601 (2006).
[17] A. P. Sokolov, U. Buchenau, W. Steffen, B. Frick, and A. Wischnewski, Phys. Rev. B **52**, R9815 (1995).
[18] T. S. Grigera *et al.*, Nature (London) **422**, 289 (2003); P. Verrocchio, J. Non-Cryst. Solids **352**, 4536 (2006).
[19] A. Monaco, A. I. Chumakov, G. Monaco, W. A. Crichton, A. Meyer, L. Comez, D. Fioretto, J. Korecki, and R. Ruffer, Phys. Rev. Lett. **97**, 135501 (2006); A. Monaco, A. I. Chumakov, Y. Z. Yue, G. Monaco, L. Comez, D. Fioretto, W. A. Crichton, and R. Ruffer, *ibid.* **96**, 205502 (2006).
[20] The BP mainly arises from the boundary of the zone edge and it is produced by the flattening in the high q limit of the quasi-transversal acoustic branch (see Refs. 21 and 22).
[21] O. Pilla *et al.*, J. Phys.: Condens. Matter **16**, 8519 (2004).
[22] B. Ruzicka, T. Scopigno, S. Caponi, A. Fortano, O. Pilla, P. Gura, G. Monaco, E. Pontecorvo, G. Ruocco, and F. Sette, Phys. Rev. B **69**, 100201(R) (2004).
[23] A. J. Martin and W. Brenig, Phys. Status Solidi B **64**, 163 (1972).
[24] V. L. Gurevich, D. A. Parshin, J. Pelous, and H. R. Schober, Phys. Rev. B **48**, 16318 (1993).
[25] N. V. Surovtsev, A. P. Shebanin, and M. A. Ramos, Phys. Rev. B **67**, 024203 (2003).
[26] A. Fontana *et al.*, J. Phys.: Condens. Matter **19**, 205145 (2007).
[27] D. Tielbürger, R. Merz, R. Ehrenfels, and S. Hunklinger, Phys. Rev. B **45**, 2750 (1992).
[28] R. Keil *et al.*, J. Non-Cryst. Solids **164/166**, 1183 (1993).
[29] R. E. Strakna and H. T. Savage, J. Appl. Phys. **35**, 1445 (1964).
[30] R. Vacher *et al.*, J. Non-Cryst. Solids **45**, 397 (1981).
[31] C. K. Jones *et al.*, Phys. Lett. **8**, 31 (1964).
[32] R. Vacher, J. Pelous, and E. Courtens, Phys. Rev. B **56**, R481 (1997).
[33] G. Baldi *et al.*, Philos. Mag. **87**, 603 (2007).
[34] R. Vacher, E. Courtens, and M. Foret, Phys. Rev. B **72**, 214205 (2005).
[35] P. Benassi, S. Caponi, R. Eramo, A. Fontana, A. Giugni, M. Nardone, M. Sampoli, and G. Viliani, Phys. Rev. B **71**, 172201 (2005).
[36] C. Masciovecchio *et al.*, Phys. Rev. Lett. **97**, 035501 (2006).
[37] G. Baldi *et al.*, Europhys. Lett. **78**, 36001 (2007).
[38] W. Schirmacher, G. Ruocco, and T. Scopigno, Phys. Rev. Lett. **98**, 025501 (2007).